minerals

MDPI

Article

Medieval Pb (Cu-Ag) Smelting in the Colline Metallifere District (Tuscany, Italy): Slag Heterogeneity as a Tracer of Ore Provenance and Technological Process

Laura Chiarantini [1,*], Marco Benvenuti [2], Giovanna Bianchi [3], Luisa Dallai [3], Vanessa Volpi [3,4] and Rosarosa Manca [2]

[1] Centro di Microscopia Elettronica e Microanalisi, Università di Firenze, Via. G. Capponi 3r, 50121 Florence, Italy
[2] Dipartimento di Scienze della Terra, Università di Firenze, Via G. La Pira 4, 50121 Firenze, Italy; m.benvenuti@unifi.it (M.B.); rosarosa.manca@unifi.it (R.M.)
[3] Dipartimento di Scienze Storiche e dei Beni Culturali, Università di Siena, Via Roma 56, 53100 Siena, Italy; giobianchi@unisi.it (G.B.); luisa.dallai@unisi.it (L.D.); vanessa.volpi@unisi.it (V.V.)
[4] Dipartimento di Biotecnologie, Chimica e Farmacia, Università di Siena, Via A. Moro 2, 53100 Siena, Italy
* Correspondence: laura.chiarantini@unifi.it; Tel.: +39-055-2757792

Abstract: Archaeological investigations of the Colline Metallifere district (Southern Tuscany, Italy) have highlighted several Medieval sites located close to the main Cu-Pb-Fe (Ag) ore occurrences. This study is focused on the investigation of late-medieval slags from Cugnano and Montieri sites using both geochemical and mineralogical methods to understand slag heterogeneities as result of ore differences and technological processes. Matte-rich slags present in both sites (with abundant matte ± speiss and frequent relict phases) represent waste products related to primary sulphide ore smelting to obtain a raw lead bullion. The distribution of slags between the Ca-rich or Fe-rich dominant composition, and the consequent mineralogy, are tracers of the different ore–gangue association that occurred in the two sites. Silver is present only in very small matte-rich slags and ores enclosed within the mortar of the Montieri site; wastes derived from silver-rich mineral charges were probably crushed for the recovery of silver. Matte-poor slags found at Montieri represent a second smelting; raw lead bullion obtained from matte slags (both Fe- and Ca-rich) was probably re-smelted, adding silica and Al_2O_3-phase-rich fluxes, under more oxidizing conditions to reduce metal impurities. This second step was probably employed for Zn-rich lead ores; this process helped to segregate zinc within slags and improve the quality of the metal.

Keywords: slags; archaeometry; archaeology; medieval; lead; zinc; silver; smelting; Tuscany

Citation: Chiarantini, L.; Benvenuti, M.; Bianchi, G.; Dallai, L.; Volpi, V.; Manca, R. Medieval Pb (Cu-Ag) Smelting in the Colline Metallifere District (Tuscany, Italy): Slag Heterogeneity as a Tracer of Ore Provenance and Technological Process. *Minerals* **2021**, *11*, 97. https://doi.org/10.3390/min11020097

Received: 15 December 2020
Accepted: 14 January 2021
Published: 20 January 2021

1. Introduction

The Colline Metallifere district (near Massa Marittima, southern Tuscany) hosts many Cu-Pb-Zn (Ag) vein deposits, which fed an important mining and metallurgical industry from the Chalcolithic period up to the 1970s. According to archaeological and historical documents, during the medieval period (12th–14th century AD), the metal production of this area was mainly focused on the extraction of copper and silver for coinage.

Archaeological campaigns of the renowned castle of Rocca San Silvestro [1,2] highlighted the presence of mining sites intrinsically connected to the process of castle formation. This aspect suggests that during the development of local seigneurships, in this geographical context, much of their economic power was based on controlling and exploiting metals.

The Colline Metallifere project, which began in the mid-1980s, aimed to study the relationships between the location of medieval settlements and mineral resources. Particular interest was focused on how local communities controlled and organized metallurgical production during the medieval period [3]. After the castle of Rocca San Silvestro, extensive research was performed on other sites with specific mining vocation, such as Campiglia

Marittima, Suvereto, Donoratico, Rocchette Pannocchieschi, Montemassi, Cugnano, and Rocca degli Alberti at Monterotondo Marittimo [4–7]. The project continued in recent years with the excavations at the site of Cugnano, with a large-scale project in the municipality of Montieri (including excavations and field surveys), and with the investigations at the alum mines site of Monteleo [8–10].

This study is focused on the analysis of slag recovered from the sites of Cugnano and Montieri. Several heaps of metallurgical slags that dated to a wide historical period (11th–14th centuries) were discovered during archaeological excavations. The slags were analyzed using optical microscopy, SEM-EDS, XRD, ICP-OES, ICP-MS and INAA with the aim of characterizing the archaeometallurgical activity performed in these sites. The data provide us with an extremely complex picture of the different metallurgical activities carried out in this area, with many aspects still to be clarified.

2. Geology and Ore Mineralogy

The Southern Tuscany area is located in a portion of the Northern Apennines orogenic belt, which is a Tertiary thrust and fold belt verging to NE-SW and resulting from the closure of the Ligurian-Piedmont Ocean and the subsequent collision between the Adria microplate and the European Plate. Within the tectonic pile, the lower units were deposited on the continental Adria Plate (the continental Tuscan Domain and epi-continental Subligurian Domain). The top units—known as the Ligurian Domain—represent sediments and portion of oceanic crust (Figure 1).

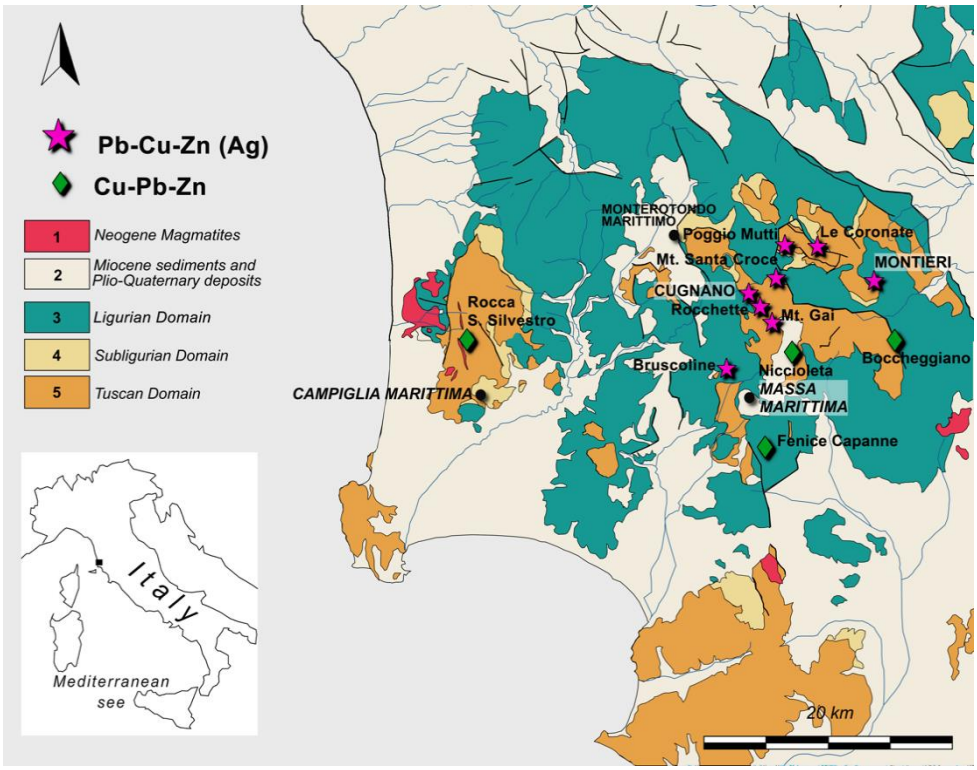

Figure 1. Schematic geologic map of southern Tuscany with locations of the main ore deposits. (1) Acid igneous or subvolcanic rocks, dykes and sills, volcanic rocks, and pyroclastic deposits; (2) conglomerates, sandstones, clays, evaporites, and sands; (3) limestones, marl, sandstones, and mudstones (late Cretaceous–Early Paleocene), shales, siltstones, and limestones (early Cretaceous), ophiolites (Jurassic); (4) sandstones, conglomerates, shales, limestones, and siltstones (Paleocene–Miocene); (5) from bottom: limestone formations, radiolarites, shales, marls, calcilutites, calcarenites, and sandstone flysh (late Triassic–early Miocene).

Metal deposits in the Colline Metallifere district are mostly characterized by Cu-Pb-Zn (Ag) vein bodies associated with late-Apenninic tectonic lineaments and emplaced by magmatic-meteoric hydrothermal fluids in the late stage of the Apenninic orogeny [11]. The more significant silver-rich mineralizations are located between Montieri and Massa Marittima (Figure 1).

Following Pratellesi [12], the mineralizations in the Montieri area generally occur as small ore veins and stockworks preferentially hosted both in sandstones and limestones of Tuscan units. The ores occurring at Poggio Mutti, Le Cornate, Mt. Santa Croce, and Mt. Gai are hosted in limestones. Only at Rocchette (near Cugnano) and Bruscoline (near Massa Marittima), polymetallic ores are hosted near the contact between the limestones of the Tuscan domain and Ligurian units.

In medieval times, ore was probably mined both by open-pit excavation (as in the area near the two castle sites of Rocchette Pannocchieschi and Cugnano) and, more frequently, by digging shafts and tunnels (underground mining). The mineral vein, in many cases already visible on the surface, was attacked in several places via shallow pits and then pursued at lower depths, where mine-working systems developed sometimes in highly complex tunnels [3,13]. The main ore mineralogy includes galena, argentian tetrahedrite, sphalerite, pyrite, and chalcopyrite in a calcite-rich gangue with gypsum, fluorite, and quartz. Unfortunately, most of the ore has already been mined. Descriptions provided by previous authors [12,14] show some minor but significant differences in ore mineralogy and phase abundance. These are shown in Table 1.

Table 1. Main ore mineralogy of investigated sites. Abbreviations: Gn—galena; Ttr—tetrahedrite; Py– pyrite; Sp—sphalerite; Ccp—chalcopyrite; Cv—covellite; Cal—calcite; Fl—fluorite; Qz– quartz; Sm—smithsonite; tr = trace; x = present; xx = abundant.

Site	Gn	Ttr	Py	Sp	Ccp	Cv	Fe-Oxhydroxides	Cu Carbonates	Gangue
Montieri	XX	XX	X	XX	tr	tr	X	X	Cal, Fl, Qz, Sm, Mn-ochre
Cugnano	XX	XX	XX		X	X	XX	X	Cal

Ore occurrences around the Montieri area are characterized by abundant argentian galena, tetrahedrite, and sphalerite, with minor pyrite, Fe-oxydroxides (limonite and goethite), Cu carbonates, and scarce Cu sulfides hosted within a calcitic gangue, often associated with fluorite, quartz, and rare Mn-rich ochre and smithsonite.

Polymetallic ores around Cugnano (Rocchette, Poggio Trifonti) are dominated by abundant argentian galena, tetrahedrite, pyrite with minor chalcopyrite, covelline, Fe-oxydroxides, and Cu-carbonates within a calcitic gangue. Explorative analyses of ore minerals performed during the 19th century in the Montieri area [15] evidenced significant silver concentration in all galena, tetrahedrite, and sphalerite-rich ores (1.5 wt%, 1.3 wt%, and 1 wt%, respectively). Similar analyses of ores around Cugnano castle indicated a fahlerz ore tennantite with about 1.6 wt% of silver [16]. More recently, lower but significant silver contents (0.2–0.4 wt%) were detected in the galena–sphalerite association from Montieri, Mt. Coronate, and Poggio Mutti, and in the galena (0.1 wt%) and galena- tetrahedrite ore (0.45 wt%) from Cugnano, confirming that argentian tetrahedrite and galena are the main silver-carriers, together with minor argentite, proustite, and pyrargyrite [12].

3. Materials and Methods

3.1. Slag-Heap Sampling: Cugnano Site

Archaeological investigations in the abandoned castle of Cugnano [17,18] located near the ore-bearing veins of Poggio Trifonti, began in 2003 (Figure 2a,b). The original part of the castle probably dates to the beginning of the eighth century.

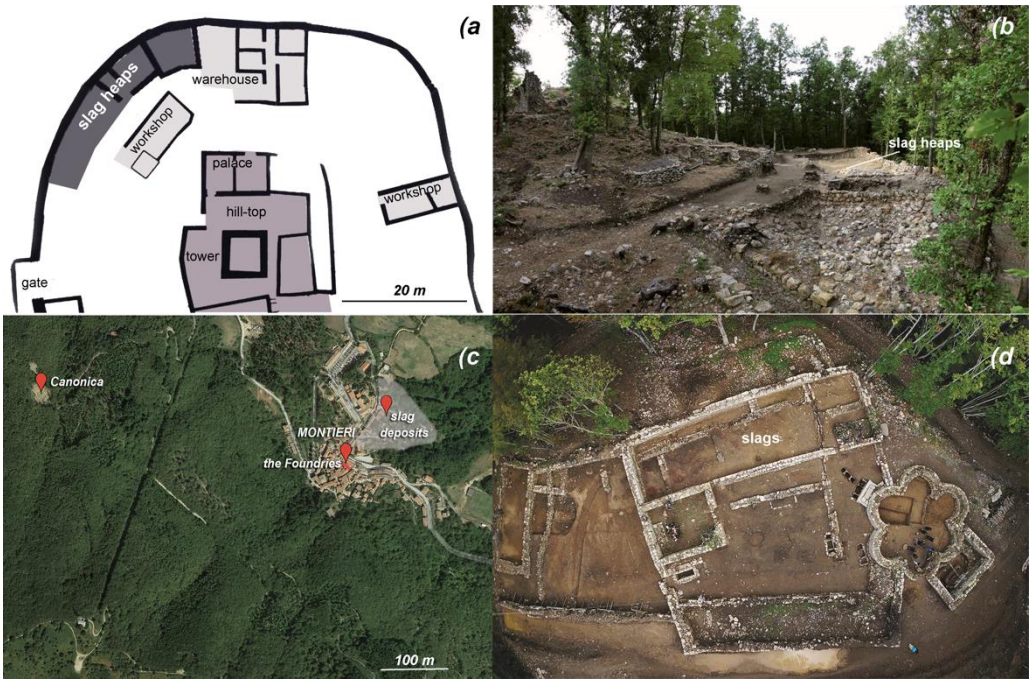

Figure 2. Topographic maps and views of investigated sites: (**a**,**b**) Cugnano; (**c**) Montieri; (**d**) Montieri, Canonica site.

At a later stage, but certainly before the 10th century, two fairly deep, pseudo-circular cavities were created outside the earliest part, which are interpreted as possible open-pit mining. The construction of a stone-built defensive wall enclosing the site can be dated to the 10th–11th centuries, while in the 12th century, a large area was probably created for ore processing on the northwest slope of the site. During the 13th century, when the castle belonged to the Aldobrandeschi family, a well-populated "borgo" developed on the opposite side of the metal-working area. In the 14th century, the castle fell within areas of Siena expansion, and it is possible that a large-scale ore processing activity was undertaken within the site [3]. This is supported by the presence of about 450 tons of slags discharged over the previous buildings, roads, and lanes within the settlement. Some scattered slags were collected from the less-abundant heaps from to the 11th-13th centuries, while most of samples (13) were collected from the large 14th century slag dump. The slags are generally large fragments of typical tapped slag with evident flowing texture and abundant, large (from millimetric to centimetric) inclusion of matte (Figure 3a,b).

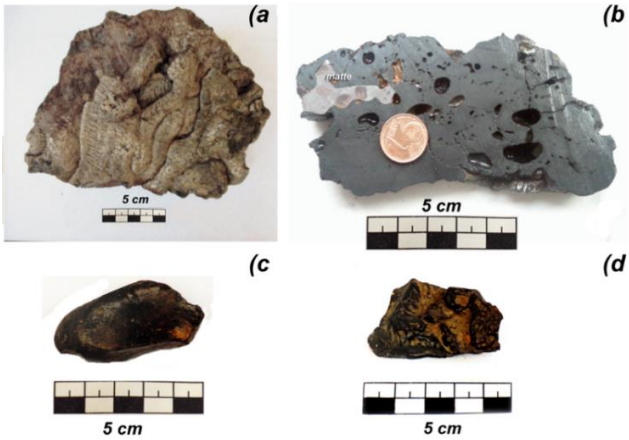

Figure 3. Macroscopic images of sampled slags: (**a**) sample from Cugnano with evident flowing texture and (**b**) abundant, large porosity and inclusion of matte (white) visible in the cross-section; (**c**,**d**) small glassy samples from Montieri with scarce flowing texture.

3.2. Slag-Heap Sampling: Montieri Site

Archaeological investigations of different sites of Montieri area began in 2007. The Bishop of Volterra was the main political figure there, and this locality was certainly at the center of a complex system of ore-working and metal production, probably connected to the activities of the neighboring castles. The importance of Montieri is documented by the presence of a mint that, between the end of the 12th century and the first half of the following century, struck coins on behalf of the Volterra bishop [19–21].

Archaeological research is currently being conducted in three different, complementary areas: the residential centre of Montieri, including the partial excavation of the large building known as Le Fonderie (The Foundries), where the bishop's mint was likely situated [22]; the slag deposits along the roads and lanes inside the ancient castle, located downstream from the current residential area of Montieri; and the Canonica site.

The latter area is located on the artificial terraces of the hill near Montieri (Poggio di Montieri, Figure 1), where documents attest to the 1133 AD existence of a parish church (Canonica) linked to the Bishop of Volterra (Figure 2c,d). The stratigraphy shows a settlement sequence spanning from the ninth to the 11th centuries, characterized by: a six apses church, a small adjacent space containing burials, and a stone enclosure bordering a central, open space with two long buildings [5]. During the 12th–13th centuries, variations were made to the existing system of structures, and only in the later 14th century was a new, residential building added to the original structures before the final abandonment of the site at the beginning of the 15th century. Outside the enclosure, there are buildings that possibly were employed for productive activities, including metallurgy, as suggested by the presence of about 300 kg of slags dated to the 13th century. Many small fragments of slags measuring up to 1.5 cm were reemployed, probably as refractory, in the white mortar used in walls and tombs dated from the 11th to 13th centuries, that support the abundance of metallurgical waste material stored on site. These remains, together with the presence of an extensive burial area, suggest that the main function of this site was connected to a metallurgical workshop, rather than to mining [3].

Few slag samples were found within the Le Fonderie building site. Five samples were selected for analyses. Four more samples were selected from the slag heaps (uncertain age) downstream the Montieri settlement. Finally, 12 samples were selected among the slag heaps found at the Canonica. These slags are generally very small fragments (up to few centimeters in length), often extremely glassy, with scarce flowing texture and absent or very scarce millimetric inclusion of matte (Figure 3c,d).

3.3. Analytical Methods

A preliminary characterization of the macroscopic features (color, streak, texture, and porosity) of all the slag samples was performed. Even if most slags were un-weathered, their superficial portions were removed before sample preparation.

All sample mineralogy was determined by optical (reflected light with polished thick and thin sections) and X-ray powder diffraction qualitative analysis. All samples were characterized using a Philips PW 3710 diffractometer with a Philips X'Pert data acquiring system, operating at 40 kV–20 mA, with Cu anode and monochromator, 2°/min goniometry speed, scanning range 2θ between 5°–75°. Due to the highly refractory nature of the slag samples, which contained large sulfides inclusions or aluminium oxides, bulk composition, as major, minor, and trace contents (Cu, Zn, As, Sb, Pb, Ag) of larger samples, was performed by means of metaborate/tetraborate fusion and ICP-MS/ICP-OES analyses combined with INAA at the Actlabs laboratories. Depending on the amount of sample, two different analytical methods were employed: (1) lithium metaborate/tetraborate fusion combined with ICP-MS measurements (detection limits: 30 ppm for Zn; 20 ppm for Cr, Ni; 10 ppm for Cu; 5 for As, Pb; 2 ppm for Ba, Sr; 0.5 ppm for Ag, Sb); (2) Sodium peroxide fusion combined with ICP-OES measurements for major/minor elements, and INAA analysis for Na and trace elements (detection limits: 500 ppm for Na; 100 ppm for Ba, Pb; 50 ppm for, Cu, Ni, Zn; 10 ppm for Cr; 5 for Ag; 2 ppm for As; 0.2 ppm for Sb; 0.1 ppm for

Sr). The entire analytical ranges are reported for each method (analytical codes: WRA + ICP—4Litho; 8-Peroxide ICP-OES; 1D-INAA) at the following link: https://cdn.actlabs.com/wp-content/uploads/2020/11/Actlabs-Schedule-of-Services-Euro.pdf. The mean bulk composition of very small slag fragments from Montieri was determined as the mean value of at least four large semi-quantitative SEM/EDS raster analyses, each covering an area of approximately 5–7 mm^2; only the major and minor element compositions were detected.

The mineral chemistry of individual phases was investigated by SEM/EDS (ZEISS EVO MA15 equipped with EDS and software OXFORD INCA 250; 15–20 kV accelerating voltage, 700 pA emission current) at the Centro di Microscopia Elettronica e Microanalisi (MEMA) of the University of Florence.

Raman spectroscopy was also employed as complementary technique to characterize some inclusions found in the slags. Micro-raman analysis was performed using a Horiba-Jobin Yvon LabRam-IR, equipped with 632 nm He-Ne Laser source, 1800 gr/mm diffraction grating spectrometer, and a Peltier-cooled 1024 × 256 CCD camera.

4. Results

4.1. Slags from Cugnano: Chemical Composition and Mineralogy

The bulk composition of the slags is reported in Tables 2 and 3. All slags from Cugnano showed similar composition and mineralogy. They were generally extremely rich in iron (as FeO: 46.8–59 wt%), with minor SiO_2 (11.1–22.7 wt%), variable CaO (4.6–17.1 wt%), and less-abundant Al_2O_3 (4.2–10.3 wt%). They also showed a significant sulfur content (0.9–3 wt%), as well as lead, copper, and minor Zn, as shown by the large and abundant matte inclusions; also relevant was the constant presence of small amounts of both As and Sb. The silver content was generally very low, always below 100 ppm, with the exception of sample S1-13022 (303 ppm).

The mineralogy was quite homogeneous as well, and strongly reflected bulk slag composition (Table 4).

The most abundant phases were iron oxides, generally wüstite in dendrites and/or in globular masses enclosing matte and/or speiss (Figure 4a); while magnetite and other oxides (hercynite) were rarer, with euhedral pseudo-cubic habitus. Silicates mostly included abundant kirschteinitic olivine (Figure 4b), generally as skeletal crystals, small needles, or chain crystals, reflecting different cooling rates [23]. Melilites, generally akermanitic (rare hardystonite), were less abundant, with anhedral habitus among olivine; silicate glass was also common among the other phases. All slags were characterized by abundant large-matte droplets, so we have classified them as matte-slag (iron rich). Matte was composted by Fe-S (similar to natural pyrrhotite) and Cu-Fe-S phases; rare Pb-S and Zn-S were found. Speiss inclusions were also common; they were generally found in bigger droplets surrounded by a cover of matte and wüstite (Figure 4c–e). Metallic phases enclosed in speiss showed generally small dimensions and were finely intermixed. However, the SEM/EDS analyses of several coarse-grained inclusions hallowed the identification of the main phases, which were: metallic Pb, metallic Sb, copper antimonide (Cu-Sb), metallic Fe, and metallic Fe-As compound (Figure 4c–e). According to the SEM/EDS analyses, the metallic lead contained about 4.5 wt% Sb, while the metallic antimony contained up to 4.6 wt% of Pb. Copper antimonide showed variable composition (Cu 46–56 wt%), with constant contents of Ni (1.5 wt%) and up to 6 wt% of Ag. Metallic Fe, particularly abundant in some samples (Figure 4d), generally contained about 5% As, while the Fe-As compound showed As contents of around 27 wt%. Metallic Ag is quite rare, but is generally associated with antimony phases and metallic Pb. Some relicts of quartz were found in the slags, and a millimetric relic of iron oxides (probably hematite) enclosed within a large mass of matte and speiss was observed.

Table 2. Chemical composition of Matte Fe-rich slags.

Site	Cugnano													Montieri			
Type	**Matte Fe Rich**	**Matte Fe Rich**	**Matte Fe Rich**	**Matte Fe Rich**	**Matte Fe Rich**	**Matte Fe Rich**	**Matte Fe Rich**	**Matte Fe Rich**	**Matte Fe Rich**	**Matte Fe Rich**	**Matte Fe Rich**	**Matte Fe Rich**	**Matte Fe Rich**	**Matte Fe Rich**	**Matte Fe Rich**	**Matte Fe Rich**	**Matte Fe Rich**
Sample	A1-13011	A2-13019	A3-13009	A3-13028	B2-13019	B3-13016	C1-13009	C1-13011	C1-13022	C1-13028	AG-13011	E-13022	S1-13022	BO2	DO1 °	BO1 *	CO1 *
SiO_2	22.75	15.96	15.98	18.51	18.75	11.11	19.02	20.28	15.46	16.20	21.41	22.66	13.91	23.68	18.36	28.0	23.5
TiO_2	0.44	0.27	0.35	0.35	0.33	0.24	0.40	0.38	0.28	0.24	0.36	0.49	0.39	0.43	0.40	n.d.	n.d.
Al_2O_3	7.68	5.24	5.83	5.75	6.25	4.18	7.26	6.44	5.39	4.60	5.80	10.26	5.67	7.64	5.59	8.7	7.0
Fe_2O_3	52.58	64.10	55.09	57.63	58.51	65.53	54.62	55.37	63.96	63.98	58.63	52.01	53.29	47.79	54.19	n.d.	n.d.
as FeO	47.31	57.68	49.57	51.86	52.65	58.96	49.15	49.82	57.55	57.57	52.76	46.80	47.95	43.00	50.56	42.2	37.1
MnO	0.39	0.32	0.35	0.36	0.24	0.20	0.46	0.32	0.33	0.24	0.23	0.47	0.19	0.67	0.44	n.d.	0.4
MgO	1.52	0.94	1.15	1.23	0.98	0.75	1.29	1.16	0.96	0.91	1.10	1.62	0.80	1.33	1.04	0.9	1.1
CaO	9.73	12.88	17.08	15.31	7.41	5.89	11.99	9.48	11.70	15.11	10.43	7.56	4.56	14.25	10.98	5.9	14.2
K_2O	2.01	1.18	1.60	1.26	1.34	1.06	1.95	2.00	1.15	1.15	1.97	1.59	1.49	1.68	1.81	2.1	1.6
Na_2O	0.26	0.22	0.21	0.24	0.19	0.16	0.30	0.34	0.17	0.20	0.31	0.22	0.15	0.48	0.69	n.d.	n.d.
P_2O_5	0.25	0.22	0.26	0.22	0.23	0.22	0.30	0.18	0.23	0.19	0.29	0.26	0.21	0.57	n.d.	n.d.	n.d.
TOT/S	1.90	1.53	1.04	1.45	1.06	3.01	2.85	2.88	2.29	0.94	1.72	1.18	1.94	2.04	2.14	6.4	5.7
F *	n.d.	n.d.	n.d.	n.d.	n.d.	n.d.	n.d.	n.d.	n.d.	n.d.	n.d.	n.d.	n.d.	n.d.	n.d.	n.d.	3.6
L.O.I.	−6.29	−6.54	−4.05	−6.23	−3.18	−10.74	−6.33	−6.27	−7.88	−6.30	−6.05	−4.80	6.30	−4.90	n.d.	n.d.	n.d.
As	0.02	0.06	0.10	0.04	0.73	2.72	0.14	0.14	0.09	0.07	0.09	0.03	1.25	0.03	0.07	0.1	1.1
Ba	0.77	1.03	0.16	1.04	0.58	0.07	0.61	0.07	1.52	0.21	0.53	0.80	0.31	0.38	<100 ppm	n.d.	n.d.
Cu	0.33	0.55	0.46	0.40	1.30	4.16	0.86	1.33	0.59	0.40	0.62	0.35	1.47	0.59	0.43	0.1	0.6
Pb	1.18	1.72	1.47	1.18	1.98	2.19	1.83	2.30	1.05	1.39	2.22	2.47	6.21	0.46	1.77	3.8	0.9
Sr	0.02	0.04	0.02	0.04	0.02	0.01	0.03	0.02	0.04	0.02	0.03	0.02	0.01	0.37	0.60	n.d.	n.d.
Sb	0.13	0.56	0.37	0.43	2.33	5.45	0.65	0.49	0.42	0.46	0.61	0.24	1.95	0.14	0.58	n.d.	n.d.
Zn	2.01	0.41	0.45	0.19	0.16	0.81	1.30	0.69	0.33	0.26	0.35	1.94	0.65	2.17	1.26	1.8	3.3
Ag ppm	3	7	7	5	62	99	33	53	7	7	11	27	303	14	<5	n.d.	n.d.
Cr ppm	80	70	50	70	80	60	80	80	80	70	70	100	50	90	<10	n.d.	n.d.
Ni ppm	30	40	40	30	190	520	40	40	40	30	80	30	210	20	80	n.d.	n.d.
TOT	97.69	100.69	97.93	99.39	99.21	97.02	99.52	97.60	98.07	100.26	100.64	99.37	100.75	99.80	100.34	100	100
V.I	2.01	3.45	3.21	2.90	2.51	4.38	2.48	2.36	3.45	3.61	2.45	1.77	2.82	1.96	2.74	1.39	1.79
Kz	2.18	3.60	3.32	3.00	2.63	4.72	2.69	2.58	3.60	3.72	2.60	1.94	3.25	2.09	2.97	1.72	2.11
ln (η) 1250 °C	0.38	0.79	0.52	0.32	0.25	2.80	0.25	0.25	0.78	0.93	0.25	0.54	0.46	0.43	0.30	0.75	0.41

° determined by sodium peroxide fusion ICP-OES and INAA; * determined only with SEM/EDS; n.d. = not determined.

Table 3. Chemical composition of Matte Ca-rich and Matte Poor slags.

Site	Montieri																
Type	**Matte Ca Rich**	**Matte Ca Rich**	**Matte Ca Rich**	**Matte Ca Rich**	**Matte Ca Rich**	**Matte Ca Rich**	**Matte Ca Rich**	**Matte Poor I**	**Matte Poor I**	**Matte Poor I**	**Matte Poor I**	**Matte Poor I**	**Matte Poor I**	**Matte Poor I**	**Matte Poor I**	**Matte Poor I**	**Matte Poor II**
Sample	**AM-01** °	**7a** °	**OG1** *	**S1** *	**OG2** *	**7b** *	**7c** *	**CO2** °	**VO1** °	**F2** *	**EO2** *	**S2** *	**AO2** *	**AO-M2** *	**4** *	**5** *	**GO2**
SiO_2	21.82	19.30	28.7	28.4	29.3	31.2	26.0	21.05	28.67	36.3	37.5	30.3	34.1	34.4	32.9	34.0	16.33
TiO_2	0.42	0.47	0.2	0.5	0.2	0.2	n.d.	0.50	0.57	0.2	0.7	n.d.	0.3	0.3	0.2	n.d.	0.58
Al_2O_3	8.98	8.28	6.3	9.8	7.8	9.3	6.6	9.67	12.91	12.6	14.5	9.4	14.9	11.9	8.6	8.4	11.45
Fe_2O_3	26.88	26.17	n.d.	n.d.	n.d.	n.d.	n.d.	29.31	22.73	n.d.	n.d.	n.d.	n.d.	n.d.	n.d.	n.d.	11.68
as FeO	24.19	23.54	13.9	19.6	16.6	15.5	27.7	26.37	20.46	21.6	18.4	23.5	21.8	23.1	22.7	21.8	10.51
MnO	1.72	1.51	1.2	1.6	0.8	0.8	1.3	1.60	0.87	0.4	1.0	1.1	1.0	1.0	1.0	2.2	12.01
MgO	1.72	1.51	1.7	1.8	1.4	1.8	2.1	1.19	1.36	1.8	1.9	2.3	1.3	1.5	1.8	2.3	1.73
CaO	22.96	22.68	29.8	29.7	32.2	27.1	22.1	21.98	14.98	16.5	15.7	20.8	16.4	15.7	24.8	17.4	13.58
K2O	1.21	1.08	1.9	1.0	1.2	2.5	0.1	0.72	2.05	2.4	2.6	1.8	2.5	2.4	1.7	3.7	0.58
Na_2O	0.19	0.13	n.d.	n.d.	n.d.	n.d.	n.d.	0.20	0.27	n.d.	n.d.	n.d.	n.d.	n.d.	n.d.	n.d.	0.14
P_2O_5	n.d.	n.d.	n.d.	n.d.	n.d.	n.d.	n.d.	n.d.	n.d.	n.d.	0.3	n.d.	n.d.	0.4	n.d.	n.d.	0.77
TOT/S	0.73	0.25	2.6	1.4	2.1	2.0	0.4	0.57	0.11	n.d.	n.d.	n.d.	n.d.	n.d.	0.7	n.d.	0.07
F *	n.d.	6.0	n.d.	n.d.	n.d.	n.d.	n.d.	n.d.	n.d.	n.d.	n.d.	n.d.	n.d.	n.d.	n.d.	n.d.	3.2
L.O.I.	n.d.	n.d.	n.d.	n.d.	n.d.	n.d.	n.d.	n.d.	n.d.	n.d.	n.d.	n.d.	n.d.	n.d.	n.d.	n.d.	10.15
As	0.11	0.1	n.d.	n.d.	n.d.	n.d.	n.d.	0.11	0.04	n.d.	n.d.	n.d.	n.d.	n.d.	n.d.	0.6	0.90
Ba	<100 ppm	<100 ppm	n.d.	n.d.	n.d.	n.d.	n.d.	<100 ppm	<100 ppm	n.d.	n.d.	n.d.	n.d.	n.d.	n.d.	n.d.	0.03
Cu	0.74	0.7	2.0	0.4	0.5	n.d.	1.1	0.88	0.47	n.d.	n.d.	n.d.	n.d.	n.d.	n.d.	0.9	0.90
Pb	3.09	5.2	4.8	1.0	8.0	n.d.	3.1	4.38	6.63	2.0	3.1	2.1	2.5	2.9	2.1	6.5	10.30
Sr	<0.1	<0.1	n.d.	n.d.	n.d.	n.d.	n.d.	< 0.1	< 0.1	n.d.	n.d.	n.d.	n.d.	n.d.	n.d.	n.d.	0.03
Sb	0.38	0.2	n.d.	n.d.	n.d.	n.d.	n.d.	0.13	0.06	n.d.	n.d.	n.d.	n.d.	n.d.	n.d.	n.d.	0.14
Zn	7.36	5.7	6.9	4.8	n.d.	9.6	9.6	6.89	6.43	6.2	4.3	8.7	5.2	6.3	3.6	2.3	5.55
Ag ppm	<5	<5	n.d.	n.d.	n.d.	n.d.	n.d.	<5	<5	n.d.	n.d.	n.d.	n.d.	n.d.	n.d.	n.d.	15
Cr ppm	30	80	n.d.	n.d.	n.d.	n.d.	n.d.	80	90	n.d.	n.d.	n.d.	n.d.	n.d.	n.d.	n.d.	110
Ni ppm	<50	<50	n.d.	n.d.	n.d.	n.d.	n.d.	<50	<50	n.d.	n.d.	n.d.	n.d.	n.d.	n.d.	n.d.	190
TOT	98.29	99.21	100	100	100	100	100	99.20	98.14	100	100	100	100	100	100	100	100.10
V.I	1.69	1.83	1.39	1.41	1.41	1.18	1.63	1.69	0.96	0.87	0.76	1.25	0.88	0.94	1.26	1.12	1.39
Kz	2.06	2.25	1.80	1.61	1.68	1.47	2.04	2.10	1.29	1.04	0.91	1.52	1.04	1.14	1.41	1.33	1.93
ln (η) 1250 °C	0.40	0.34	0.67	0.88	0.79	1.05	0.47	0.40	0.30	1.76	2.02	1.00	1.77	1.59	1.14	1.27	0.60

° determined by sodium peroxide fusion ICP-OES and INAA; * determined only with SEM/EDS; n.d. = not determined.

Table 4. Mineralogy of slags. Abbreviations: Kir—kirschsteinite; Mt—monticellite; Lrn—larnite; Mll—melilites; Wus—wüstite; Mag—magnetite; Hc—hercynite, Qz—quartz; Cls—celsian; Aug—augite; Spl—zoned spinels; Kfs—k-feldspati; Px—pyroxenes; Csp—cuspidine.

Cugnano		Main Phases			Minor Phases		Additional Phases
	Sample	**Silicates**	**Oxides**	**Matte**	**Metals**	**Speiss**	
matte Fe rich	**A1-13011**	Kir, Mtc	Wus	Fe-S; Pb-S; Zn-S	Pb	Sb; Cu-Sb	Pb oxides
matte Fe rich	**A2-13019**	Kir, Mll	Wus, (Mag)	Fe-S	Pb	Cu-Sb	Pb oxides
matte Fe rich	**A3-13009**	Kir, Mll	Wus, (Mag)	Fe-S	Pb	Cu-Sb	Pb oxides
matte Fe rich	**A3-13028**	Kir, (Mll)	Wus, (Mag)		Pb	Sb; Cu-Sb	
matte Fe rich	**B2-13019**	Kir	Wus	Fe-S	Pb	Fe-As; Cu-Sb	Pb oxides
matte Fe rich	**B3-13016**	Kir	Wus, (Hc)	Fe-S; Cu-Fe-S; Zn-S	Pb	Fe; Fe-As; Cu-Sb	Pb oxides, hematite
matte Fe rich	**C1-13009**	Kir	Wus, Mag	Cu-Fe-S; Pb-Zn-S	Pb; Cu	Cu-Sb	
matte Fe rich	**C1-13011**	Kir	Wus, (Mag)	Cu-Fe-S	Pb; Cu	Cu-Sb	Qz,
matte Fe rich	**C1-13022**	Kir, Mll	Wus	Cu-Fe-S; Fe-S	Pb	Sb; Fe-As; Cu-Sb	Pb oxides, Fe-hydroxides, Qz
matte Fe rich	**C1-13028**	Kir, Mll	Wus, (Mag)		Pb	Sb; Cu-Sb	
matte Fe rich	**AG-13011**	Kir	Wus	Fe-S	Pb	Sb; Cu-Sb	Pb oxides
matte Fe rich	**E-13022**	Kir	Hc, (Wus)	Pb-S; Zn-S	Pb	Sb; Cu-Sb	
matte Fe rich	**S1-13022**	Kir	Mag, (Wus)	Cu-S; Fe-S	Pb	Fe-As; Cu-Sb	Pb-Sb oxides, Fe-hydroxides, Cls
Montieri							
matte Fe rich	**BO2**	Kir, (Aug)	Wus, (Spl)	Cu-Fe-S; Fe-S; (Zn-S)	(Pb)	Fe; Sb; Fe-As; Cu-Sb	Pb oxides
matte Fe rich	**DO1**	Kir, Mll	Wus	Cu-Fe-S; Fe-S; Pb-S	Pb	Fe; Sb; Fe-As; Cu-Sb	Pb oxides, Pb carbonates
matte Fe rich	**BO1**	Kir	Wus, (Slp)	Cu-Fe-S; Fe-S	Pb	Fe-As	Pb oxides; Kfs
matte Fe rich	**CO1**		Wus, (Spl)	Cu-Fe-S; Fe-S; (Zn-S)	(Pb)	Fe-As	Pb oxides
matte Ca rich	**AM-01**	Mll, Kir, (Aug)	Wus, (Spl)	Cu-Fe-S; Zn-S; Pb-S; Pb-Sb-S	(Pb)	Cu-Sb; Ni-Sb	Qz, Al_2O_3-phase
matte Ca rich	**7a**	Mll	Spl, (Wus)	Cu-Fe-S	(Pb)		Qz, Al_2O_3-phase
matte Ca rich	**OG1 ***	Px, Csp	Spl, (Wus)	Cu-Fe-S; Cu-S; Zn-S; Pb-S	Pb	Cu-Sb; Ni-Sb; Sb	Al_2O_3-phase
matte Ca rich	**S1**	Px, (Csp)	Spl, (Wus)	Cu-Fe-S; Cu-S; Zn-S; Pb-S	(Pb)	Cu-Sb; Sb	Fe-hydroxides, calcite, Qz
matte Ca rich	**OG2**	Csp, Mll	Spl, (Wus)	Cu-Fe-S; Zn-S; Pb-S	(Pb)	Cu-Sb; Ni-Sb	Al_2O_3-phase
matte Ca rich	**7b**	Mll, (Csp)	Spl	Cu-Fe-S; Fe-S	(Pb)	Cu-Sb	Qz, Al_2O_3-phase; ZnO
matte Ca rich	**7c**	Mll	Spl, (Wus)	Cu-Fe-S	(Pb)		Qz

Table 4. *Cont.*

Cugnano		Main Phases			Minor Phases		Additional Phases
	Sample	**Silicates**	**Oxides**	**Matte**	**Metals**	**Speiss**	
matte poor I	**CO2**	(Mll)	Spl	(Cu-S)	Pb		Al_2O_3-phase
matte poor I	**VO1**	(Px)	Spl	(Cu-S, Cu-Fe-S)	Pb	Sb	Al_2O_3-phase
matte poor I	**F2**	(Px)	Spl	(Cu-S, Cu-Fe-S)	Pb		Al_2O_3-phase
matte poor I	**EO2**		Spl	(Cu-Fe-S)	(Pb)	(Ni-Sb)	Al_2O_3-phase
matte poor I	**S2**	(Mll)	Spl	(Cu-Fe-S; Zn-S)	Pb	Sb; Ni-Sb	Al_2O_3-phase
matte poor I	**AO2**		Spl		(Pb)		Al_2O_3-phase
matte poor I	**AO-M2**		Spl	(Cu-S)	Pb	As-Sb	Al_2O_3-phase
matte poor I	**4**	(Px)	Spl	(Cu-Fe-S; ZnS)	Pb		Al_2O_3-phase
matte poor I	**5**	(Px)	Spl	(Cu-Fe-S; Cu-S)	Pb	Sb	Al_2O_3-phase
matte poor II	**GO2**	Csp, Lrn, (Aug)	Spl, (Mn-oxide)	(Cu-S)	Pb (Cu)		Al_2O_3-phase

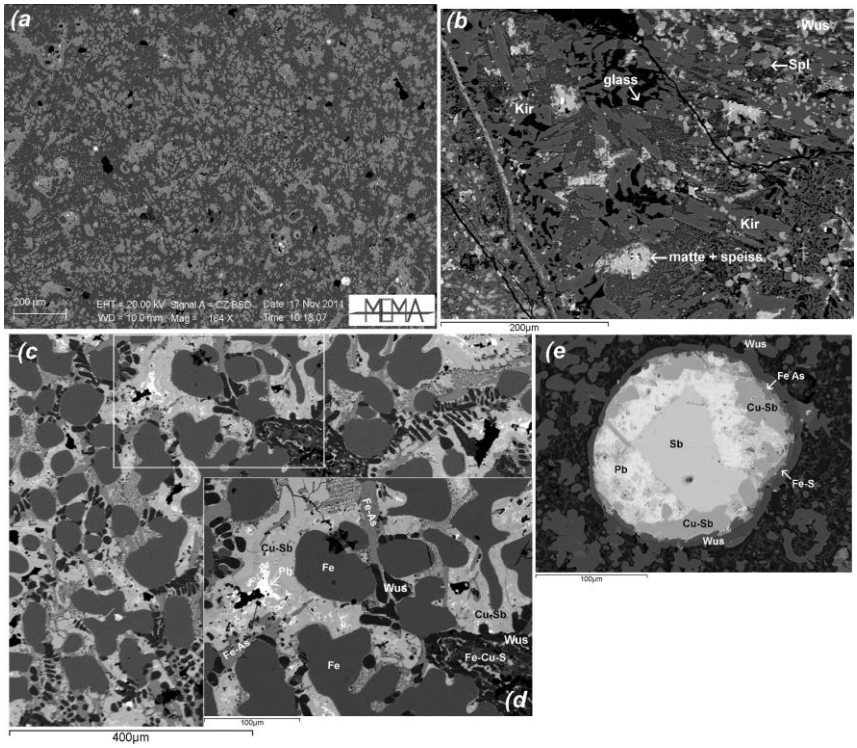

Figure 4. Backscattered electron (BSE) images of Fe-rich matte slags from Cugnano: (**a**) panoramic view with wüstite dendrites (medium grey); (**b**) kirschteinitic olivine, glass, wüstite/spinels, and matte/speiss inclusions; (**c**) particular of a matte/speiss inclusion with many metallurgical sulfides and metals, enlarged in (**d**); (**e**) Pb droplet with Sb and Cu-Sb phases. Abbreviations: Kir—kirschsteinite; Wus—wüstite; Spl—zoned spinels.

4.2. Slags from Montieri: Chemical Composition and Mineralogy

The slags collected in the Montieri area differed from the Cugnano site, independently from the collection site and supposed age, and were extremely heterogeneous in both chemistry and mineralogy (Tables 2–4). Four groups originating from the entire collection area can be schematically identified.

The first group was very similar to the Cugnano matte-slag (Fe-rich) group, except for slightly higher SiO_2 (18.4–28 wt%) and Zn contents (1.2–3.3 wt%). They also showed similar mineralogical assemblage, with more abundant zoned spinels (hercinite-magnetite) and less abundant smaller matte/speiss inclusions.

The second group was classified as matte slag (Ca-rich), since the samples displayed abundant matte inclusions (up to a few mm in length) and bulk composition distinctly enriched in CaO (22.1–32.2 wt%) with respect to Cugnano. They were also lower in FeO (13.9–27.7 wt%) and slightly higher in both Al_2O_3 and SiO_2. They also displayed significant Zn content (up to 9%), while As and Sb were hardly detected (Tables 2 and 3).

The mineralogy was characterized by a heterogeneous assemblage of several silicates, which comprises mostly anhedral pyroxenes, similar to natural augite or more commonly with diopside-hedenbergitic composition (containing up to the 7 wt% ZnO) and elongate prismatic crystals of cuspidine ($Ca_4(Si_2O_7)(F,OH)_2$) (Figure 5a). Anhedral Ca-rich melilites were also common (from hardystonite to gehlenite like), while rare elongated kirschteinitic olivine were observed in some samples. Oxides were mostly skeletal or sub-euhedral spinels strongly zoned, with an Al-Fe composition in the core (hercynite-like), Fe-rich rims (magnetite-like) and significant Zn contents (up to 10 wt% ZnO) (Figure 5a). Wüstite dendrites were rare.

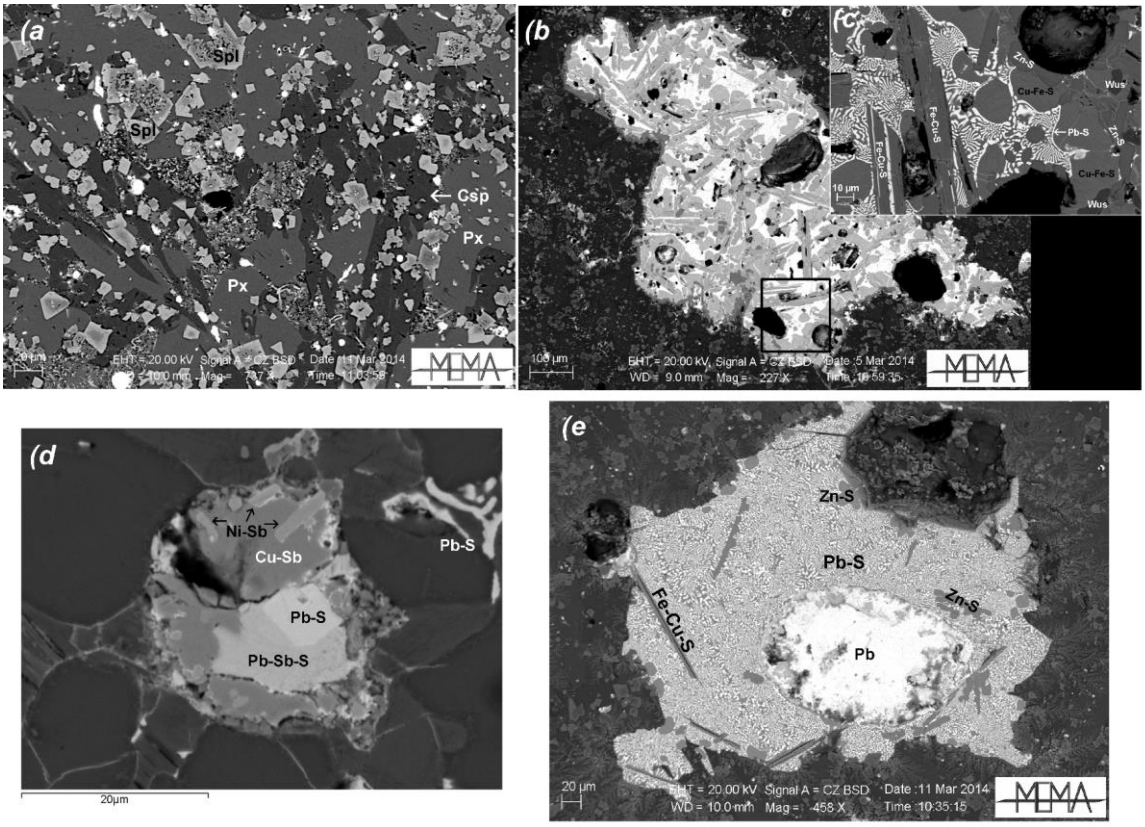

Figure 5. BSE images of Ca-rich matte slags from Montieri: (**a**) panoramic view with pyroxenes, cuspidine, and zoned spinels, (**b**) particular of a matte/speiss inclusion with many metallurgical sulfides and metals, enlarged in (**c**); (**d**) matte/speiss inclusion with Cu-Sb and Ni-Sb phases; (**e**) Pb droplet surrounded by matte. Abbreviations: Px—pyroxenes; Csp– cuspidine; Wus—wüstite; Spl—zoned spinels.

Matte inclusions are made by Cu-Fe-S (similar to natural chalcopyrite and/or idaite), with abundant Pb-S and Zn-S phases; Cu sulfides (similar to natural covellite and chalcocite) and Pb-Sb-S phases are less common (Figure 5b,c). Small speiss inclusions were observed in bigger droplets surrounded by a cover of matte; phases generally included metallic Pb (with traces of Ag up to 0.5 wt%), copper antimonide (Cu-Sb), and nickel-antimonide (Ni-Sb) (Figure 5d,e). Some relicts of Fe-hydroxides masses associated with calcite were occasionally found, and resorbed masses composed by an Al_2O_3-phase (see description below) were detected.

The third group of slags was completely different from the previous ones. They were mostly glassy, with scarce or absent matte inclusions, and are called matte-poor slags (I). Their bulk composition was characterized by very high SiO_2 contents (21–37.5 wt%); significant FeO (18.4–26.4 wt%), although lower than the matte (iron-rich) group; CaO (15.7–24.8 wt%); and high Al_2O_3 contents (8.4–14.9 wt%). Zn contents were among the highest identified in the slags (2.3–8.7 wt%), and significant Pb concentration also was detected (2–6.6 wt%). All the other metals, including silver, were almost absent.

As mentioned previously, this group of slags was mostly made by a glassy groundmass where only scanty silicate phases are observable; they were generally pyroxenes (petedunnite or diopside-hedenbergite like), or more rarely, melilites (hardystonite or akermanite) (Figure 6a,b). Glass composition generally resembled the slags' bulk composition, with higher SiO_2 (37.6–40.5 wt%) content and lower FeO (16.3–20.5 wt%) content; the glass was always rich in Al_2O_3, Zn and Pb (up to 6.9 and 5.5 wt%, respectively), and trace amounts of As (0.3 wt%) were common. The glass showed different shades of grey (Figure 6a) in backscattered images, indicating, especially around spinels, low levels of Zn and Pb. Abundant, small, zoned spinels were observable in the glassy groundmass, which

is very common in other medieval slags of Pb-Ag smelting [24]. They were euhedral or skeletal, generally with an Al-rich core (hercynite like) and Fe-rich rims, and they were commonly enriched in Zn (gahnite like), especially in the core, where ZnO contents can reach up to 20 wt% (Figure 6c). All these slags were characterized by the presence of abundant, large (observable also to the naked eye) relicts of an Al_2O_3-phase, which appears either as porous anhedral masses or as prismatic/rhombohedral crystalline aggregates (Figure 6c–f). The SEM/EDS analyses evidenced the presence of only Al_2O_3 in these phases, and the preliminary Raman analyses, which were performed on larger aggregates, identified these aggregates as being made of α-Al_2O_3. All these relicts were partially resorbed, and were always rimmed by neo-formed zoned spinels extremely enriched in Zn (ZnO up to 27 wt%) (Figure 6c,d).Common relicts of quartz were also identified. Abundant droplets of metallic Pb were scattered through the glassy matrix, with occasional trace amounts of Ag. Matte and speiss inclusions are extremely rare, and phases are difficult to identify. The matte includes Cu-Fe, Cu, and Zn sulfides, while metallic Sb and Ni-Sb were occasionally detected.

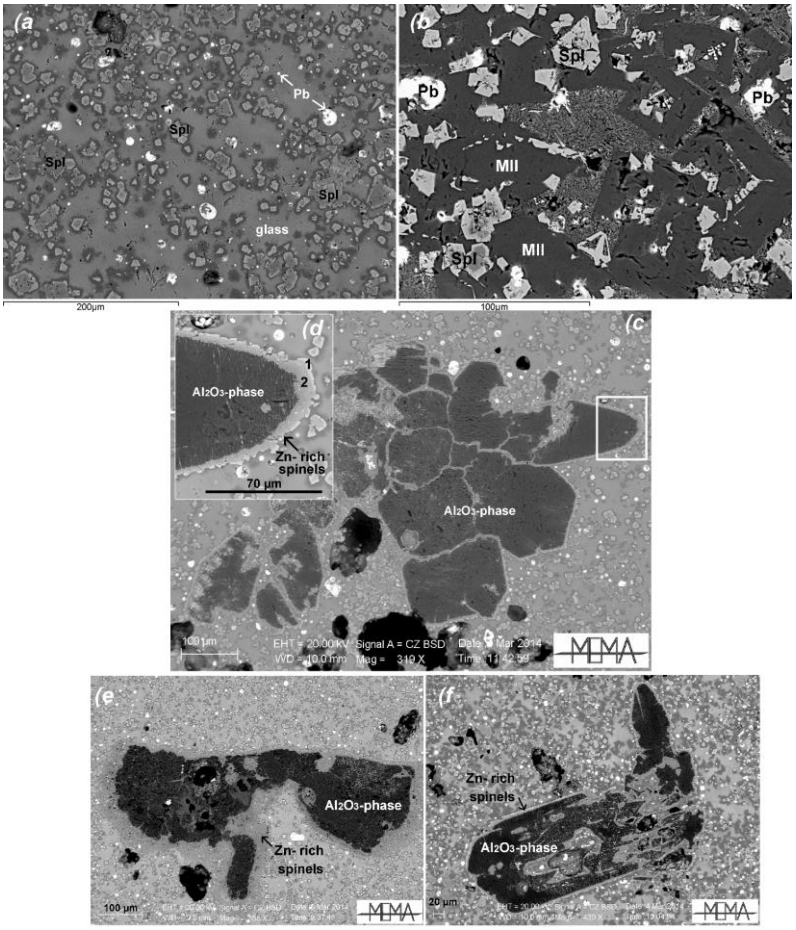

Figure 6. BSE images of matte poor slags (I) from Montieri: (**a**) panoramic view with glass, zoned spinels, and metallic lead (white droplets); (**b**) melitites and zoned spinels; (**c**,**d**) images of Al_2O_3-phase inclusions rimmed by spinels with (1) white Fe-rich rim, (2) grey Zn-rich rim; (**e**,**f**) images of Al_2O_3-phase inclusions rimmed by spinels. Abbreviations: Mll—melilites; Spl—zoned spinels.

Finally, one sample (GO2), called a matte-poor slag (II), differed from the others in both composition and mineralogy. It was characterized by a high CaO content (13.6 wt%), SiO_2 (16.3 wt%), MnO (12 wt%), and volatiles with low FeO (10.51 wt%). Al_2O_3 and Zn were in the range of matte-rich slags from Montieri, while very high Pb (10.3 wt%) and F contents (3.2 wt%) were also found.

The sample was a fine-grained mixture of Ca-rich silicates, similar to natural cuspidine and larnite, with rare pyroxenes (augite like) and abundant zoned Al-Fe spinels, which are generally enriched in both Zn and Mn (up to 26 wt% MnO) (Figure 7). Occasional dendrites of Mn-oxides (Zn rich) were observed. Extremely small droplets (<10 μm) of metallic Pb and Cu were observable among silicates, while larger masses (Figure 7) and droplets contained mostly a mixture of Pb-oxides, which displayed trace contents of Bi and Ag (0.9 and 0.4 wt%, respectively). Matte inclusions were extremely rare (Cu-S phases), and speiss was absent. Some resorbed relicts of Al_2O_3-phase were observed.

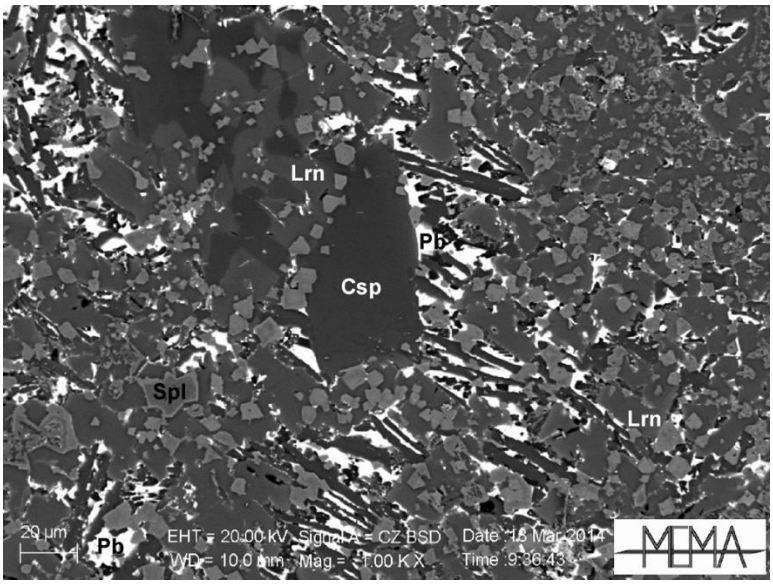

Figure 7. BSE image of a matte poor slag (II) sample from Montieri with cuspinine, larnite, zoned spinels and metallic lead. Abbreviation: Lrn—larnite; Spl—zoned spinels; Csp—cuspidine.

The entire silver content of Montieri slags was lower than those from Cugnano, and never exceeded 15 ppm. These low-Ag waste products do not support a Pb-Ag bearing-smelting process.

The most significant traces of silver were detected among the small slag fragments of building mortar from the Canonica site. No ore residues were detected among the slag heaps, whereas the tiny inclusions in the mortar generally included several ore charge fragments, mostly characterized by pyrite, iron hydroxides, sphalerite, and occasionally galena crystals with inclusions of the proustite-pyrargyrite series (Figure 8), together with silver-rich tetrahedrite (up to 5 wt% Ag) and argentite.

Slags were also present in the mortar, but due to the small dimensions of the fragments, an exhaustive characterization was not possible. However, the identified mineralogical phases and the estimated (SEM/EDS) bulk composition supported Ca-rich and Fe-rich matte slags. The entire mineralogy and textures did not differ from the two types of slags described before. Samples were characterized by several silicates and oxides, matte inclusions, and some speiss inclusions surrounded by a cover of Cu matte. Speiss are made by fine intergrowths of copper antimonide, nickel-antimonide, and metallic Pb that contains up to 5.4 wt% of silver.

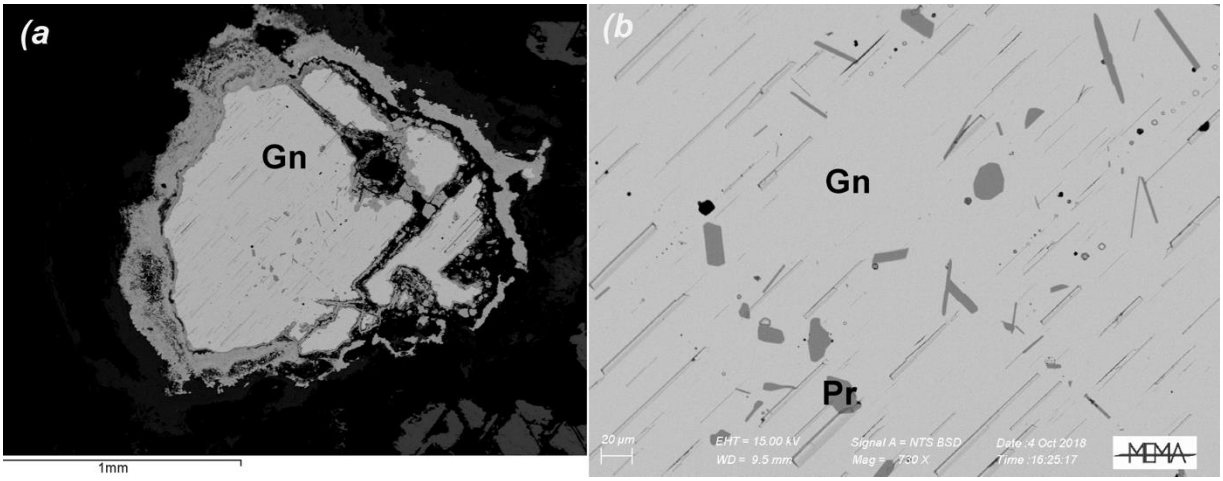

Figure 8. BSE images of ore fragments within mortar from Montieri showing galena (**a**) with proustite-pyrargyrite inclusions, enlarged in (**b**)Abbreviations: Gn = galena; Pr = proustite-pyrargyrite.

5. Discussion

The significant differences in both chemical and mineralogical composition observed in the slags of the two archaeological sites reflect the heterogeneity of the raw ore material that was used. While samples from Cugnano were quite homogeneous, those collected at Montieri were extremely heterogeneous. Different metallurgical processes performed in this area, which possibly collected and treated raw ores from a wider mining district with a more variable mineralogy, could account for this heterogeneity.

The slag bulk compositions plotted in Figure 9 show the slags' heterogeneity and an approximate estimation of the liquidus melting temperatures. Data from literature for Pb slags from the Rocchette and Arialla sites in the Colline Metallifere area [25–27] were also plotted for comparison. Due to the complex chemical composition of slags and the common occurrence of disequilibrium conditions during smelting operations, the estimated liquidus melting temperatures are to be taken with extreme caution [28,29]. Several errors could arise from the use of the SiO_2–FeO–CaO ternary diagram for these slags. Errors could occur due to the iron contents reported only as FeO, and due to significant spinels (magnetite-like) detected in the slags that could contribute Fe. An overestimation of the liquidus temperature can also arise due to the abundant presence in some slag typologies of unreacted/partially reacted quartz and Al_2O_3-phase masses, which apparently increase the slag silica bulk content and thus the estimated temperature [30]. Taking all this into consideration, lower temperatures (1150–1280 °C, with the exception of B3-13016 extremely rich in FeO) can be estimated for both the Cugnano and Montieri matte slags (Fe-rich), which are very similar to those reported for Rocchette and most of Arialla [25–27]. Higher temperatures, up to 1300–1350 °C, can be estimated for matte slag (Ca-rich) and matte-poor slags (I) and (II); these are probably less realistic, since the highest temperature level in ancient metallurgical slags has been generally estimated at about 1300 °C [31].

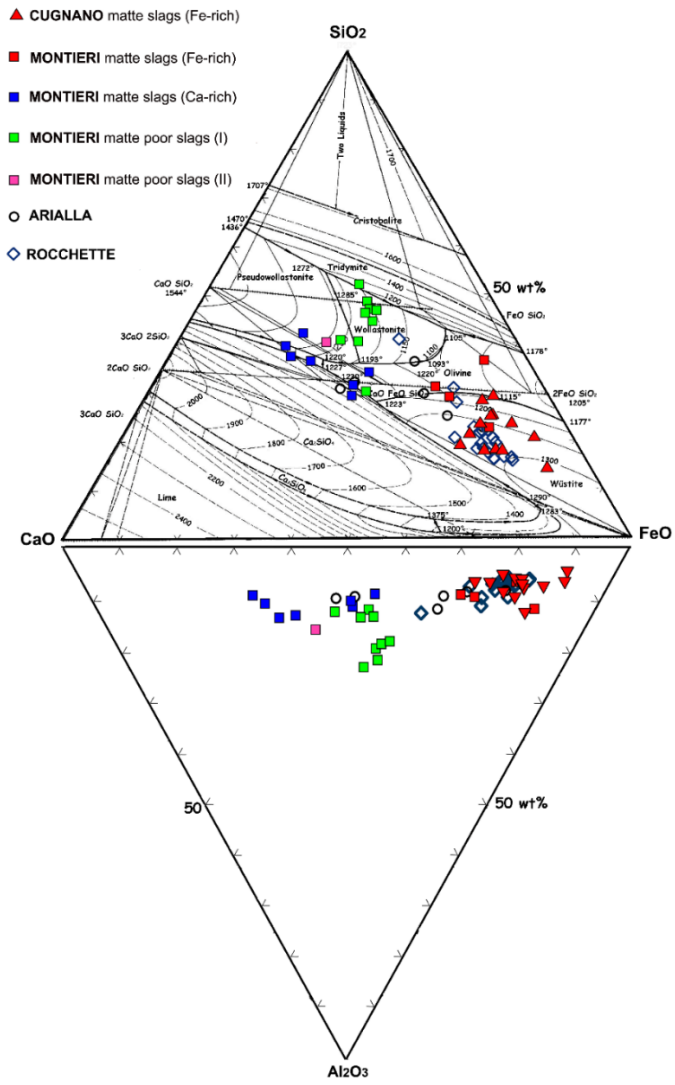

Figure 9. Chemical composition of slags into CaO-SiO_2-FeO (after Osborn and Muan [32]) and CaO-Al_2O_3-FeO diagrams (composition as wt%).

An estimate of slag viscosity is provided in Tables 2 and 3 that uses the viscosity index (v.i.), reported by Bachamann [33] and employed by previous authors [26]. The modified index (Kv cf. Bachmann et al. [34]) which also includes ZnO and PbO contents, and is considered more appropriate for our samples. Viscosity, calculated at 1250 °C for all slags, generally increases, moving from matte slag (Fe-rich)-(Ca-rich), to matte-poor slags in parallel with the increasing contents of SiO_2 and Al_2O_3 in slags.

5.1. Matte Slags

Matte slags, which occurred in both the Cugnano and Montieri sites, were all characterized by abundant matte (±speiss) inclusions up to several centimeters in length (Figures 4 and 5), but displaying variable mineralogical composition (from iron, copper-iron, and lead sulfides at Cugnano to dominant lead, zinc, and copper-iron sulfides at Montieri); abundant iron oxides mostly as reduced species (wüstite); and frequent relict phases like Fe-hydroxides and oxides, probably representing residues of gangue ± ore charge (common among Montieri and especially Cugnano ore association; see Table 1).

Silver content in all slags was so low that we wondered whether the metallurgical process was connected to silver extraction. The whole set of compositional and mineralogical features seems to suggest that they all could represent waste products related to a sort

of primary sulfide ore smelting aimed at obtaining a raw lead bullion (probably highly impure in Cu, Zn, Sb, As, and possibly Ag).

As illustrated in the two diagrams of Figure 9, the distribution of matte slags along the CaO-FeO axis could represent the different ore–gangue association that occurred in the Cugnano and Montieri areas. All matte slags from Cugnano, and only few samples from Montieri (matte slag Fe-rich), were located near the FeO edge, and could reflect the Fe-rich ore association (Table 1) typical of the Cugnano site, characterized by tetrahedrite and galena, and by lower amounts of pyrite and Fe-hydroxides. Matte inclusions detected in slags also seemed to reflect the ore mineralogy. The presence of the abundant speiss with metallic Fe, Fe-As, metallic Sb, and copper antimonide (with up to the 6 wt% of Ag) implies that the employed ore should have contained a significant amount of chemically bound Fe, Sb, and As. Similar slags and matte/speiss phases were recognized at the Rocchette site [26,27] a few kilometers away from Cugnano, where the same type of ore was probably exploited.

Silver appeared to be only an impurity in most matte-rich slags. It was generally trapped in antimony speiss phases; in fact, speiss formation is considered as an unfavorable process in silver recovery [35]. If silver extraction was one of the purposes of the smelting operations, the formation of speiss could have been partially reduced to promote the formation of iron silicate phases [35]. This seems to have been tentatively performed in the sites we studied, since abundant fayalite and common magnetite was found in matte slags. However, a variable redox condition should have been achieved during smelting, as testified by the coexistence of magnetite, wüstite, and metallic iron. The presence of active sulfur also can reduce speiss formation by promoting the formation of copper and iron sulfides rather than metallic speiss [35]. As deduced from the analyzed slags, enough sulfur was probably left in the ore to allow the matte formation. We therefore infer that the sulfide ore charged into the furnace was only partially roasted.

Many of the Montieri slags differed from Cugnano samples. They were Ca-rich matte slags located close to the Ca axis (Figure 9), with slightly higher SiO_2 contents probably reflecting a more Ca-Si-rich ore gangue association. The Montieri ore association was generally poorer in iron sulfides and hydroxides, and richer in calcite, quartz, and fluorite (Table 1) compared to the Cugnano ores. This explained the common presence of Ca-rich silicates (olivine, pyroxenes, and melilites) and the occurrence of a fluorine-bearing calcium silicate (cuspidine) that is uncommon among ancient slags [33]. As in the previous case, matte phases reflect ore mineralogy; speiss are in this case generally rare, confirming the galena-sphalerite association probably represents the more common ores. For these slags, a partially roasted ore should be charged in the furnace, and despite speiss being less abundant, more oxidizing conditions should have been employed during smelting, since metallic iron was not observed, and wüstite was definitely rarer than spinels. This type of slag has only been found in the Montieri area, even though some similarities (Figure 9) have been observed in two Pb slags from the Arialla site, as reported by Manasse and Mellini [26]. Silver content was extremely low in most of these slags. Moreover, even if a significant amount of Zn is trapped in slag (see bulk content) both as silicate (hardystonite and pyroxenes) and spinel phases due to the employment of more oxidizing conditions, the main impurity of the Pb bullion was probably zinc.

Slag samples from mortar at the Canonica site were similar to the large matte slag samples (matte slags), with the only exception being their silver contents. Silver was not detected in the bulk composition, but was easily detectable in many metallic Pb droplets. It has been never observed in large samples taken from the main waste dumps. Considering that the presence of both Ag-bearing ore fragments and metallic silver seemed to be restricted to small slags enclosed within mortar, and that those slags did not differ in mineralogy and textures from the bigger cakes from dumps, we suggest that this ore and slag association derived from the treatment of an Ag-enriched mineral charge. It is possible that silver-rich slags and ores residues were finely crushed for a proper recovery of all Ag-rich matte/metals, and then re-employed as temper in mortar. The crushing of Pb-Ag

slags for metal recovery and slag recycling is a common and well-documented practice in many medieval sites for silver extraction [36]. Even if slags have been detected in all the mortars in both tombs and structures of Canonica site, the richest Ag samples were concentrated in the structure from the 12th–13th centuries.

5.2. Matte-Poor Slags

We found no evidence that the raw Pb bullion produced at Cugnano underwent any post-smelting depuration or cupellation processes. Except for the mentioned slags, no other metallurgical wastes, such as refinement slags or litharge, were found in other coeval sites [36,37]. No fragments of crucible or cupellae have ever been found in the site. The other sporadic slags collected in different parts of the castle and belonging to various chronological horizons (11th–13th centuries; not reported in the paper) are very similar in mineralogy and composition to the described slags, suggesting that any sort of metal refinement was probably performed elsewhere.

However matte-poor slags, which were scattered throughout the Montieri territory, were mixed with matte-rich samples, suggesting that a sort of second step of ore smelting was commonly performed in this area. The more striking features of these slags were the scarcity (absence) of matte/speiss inclusions, the absence of ore charge relicts, the presence of common lead and Al_2O_3-phase inclusions, and the predominance of glass (rich in SiO_2 and Al_2O_3).

The entire set of features (especially the simultaneous absence of matte and abundancy of lead) suggests that they could be waste material associated with a type of depuration process of the raw Pb metal bullion. Their composition can be distinguished in the two diagrams shown in Figure 9 due to the high content of both SiO_2 and Al_2O_3. Their bulk composition and mineralogy suggest that the raw Pb (Ag-poor?) bullion obtained from matte slags (both Fe- and Ca-rich) was probably re-melted at Montieri, adding some Si-rich fluxes under more oxidizing conditions to reduce metal impurities. The oxygen fugacity of the process was buffered by the absence of wüstite among the iron oxides, while temperatures should be similar of those archived during matte-slag smelting, even if they seem to be overestimated due to the presence of unreacted Al_2O_3-phase grains. Only one sample of matte-poor slags (II) (GO2) strongly differed from the others, mainly due to its high CaO content. Similar to the rest of the matte-poor slags, CaO was scarce in the matte/speiss inclusions, while lead inclusions and relicts of Al_2O_3-phase were common. We inferred that this represents the residue of the refinement process of a raw lead bullion derived from a very rich Ca-rich ore, but due to the singularity of the sample, more data will be necessary to prove this hypothesis.

Whether this possible second step of smelting was performed for all the lead bullion, or if it was applied only to Ag-poor lead, is still unclear. All the matte-poor slags were Ag-poor, and the presence of silver in metallic Pb was never detected. It is therefore possible that this refinement process was applied only to matte obtained from highly impure ores. It is also possible that the Ag-rich matte recovered from the crushing of slags, like those within mortar from Canonica, was processed in a different way at the site, or processed elsewhere. The use of different and separated processes for different kind of ores (Ag-rich and Ag-poor) is strongly documented in medieval iconography, and also is supported by on-site investigations, as demonstrated by Rehren [35] for the medieval site of Altenberg in Westphalia, Germany.

5.3. Al_2O_3 Aggregates as Tracers of Depuration Process

One of main questions about matte-poor slags is: What are the function and origin of the unreacted Al_2O_3-grains? Three hypotheses can be suggested, but none of them is fully satisfactory. The first and least-realistic theory is that they represent unreacted fragments of ore-gangue charge, since Al-rich phases were not found among Montieri ores (Table 1), and no other relicts of charge minerals (like Fe-oxides) or partially smelted sulfides (matte) were detectable in significant amounts in the matte-poor slags. Second, we suggest that they could represent some portions of refractory (Al-rich) material from

furnace walls or crucibles, among which Al-rich clay minerals (like mullite) have been commonly documented for the Middle Ages [38]. Such refractory portions could have been partially absorbed in slags during melting, as occurred in ancient and modern processes [39]. If this were the case, they should have been observed only in some slag portions (close to refractory), even though Al_2O_3-phases are dispersed throughout the whole samples.

The third hypothesis is that they represent a sort of "fluxing agent" that was intentionally added during the melting. It is not clear for what purpose a high refractory phase, which surely did not lower the slag melting point, should have been added during the refining process. Some suggestions arise from modern zinc blast furnace metallurgy, in particular the papers by Zhao et al. [40,41] that deeply investigate the ZnO-FeO-Al_2O_3-CaO-SiO_2 system and the influence of Al_2O_3 contents on the systems' equilibria. The first effect of the presence of alumina is the formation of the spinel phase in the slag, which is not observed in alumina-free slags [40]. A confirmation of this evidence is that all the Al_2O_3-phase relicts were rimmed by neo-formed, Zn-rich, zoned spinels. Following Zhao et al. [41], the formation of a solid spinel in zinc metallurgy slags is an undesirable event for two main reason: (i) it increases the viscosity of slag by removing ZnO, FeO, and Al_2O_3 and increasing SiO_2 in the remaining liquid, and the spinel phase itself increases the slag viscosity favoring the tendency for blockage during slag tapping; and (ii) the Zn-rich spinel phase fixes zinc in the slag's solid phases, making it difficult to reduce and remove by vaporization, thus increasing the zinc loss in the slag.

The increased viscosity in matte-poor slags is evidenced by the calculated viscosity (Tables 2 and 3). The possibility of fixing zinc in the slag (in glass, silicate phases, and spinels) would be a desirable effect in lead (Ag) metallurgy, since it could help to reduce the zinc impurities in the bullion. There was a positive correlation between Al and Zn content in slags, and some Al_2O_3 phase relicts were also observable in Ca-rich matte slags that displayed the highest zinc content, while they were never observed in Cugnano slags, where the zinc content was generally below 1 wt%. We suggest that the practice of adding Al_2O_3-phase as a fluxing agent during smelting (matte slags) and, more commonly, during the refining processes (matte-poor slags), could help to reduce zinc impurities in the produced metal, and that this was performed especially in those areas (e.g., the Montieri site) where lead- and silver-bearing phases were closely mixed with zinc minerals. Since no traces of cupellation process were found on the site, we can suppose that this refinement process was performed prior to Pb-Ag separation, or more probably, it was dedicated to Ag-poor lead bullion obtained from impure ore. In both cases, the a high zinc content in lead was undesirable because it produced a more-impure metallic lead, and because in silver separation, the cupellation step was an unavoidable process (directly after Pb-Ag bullion for silver bearing galena, or after Cu-Ag liquation for Ag-rich fahlerz ores), and it was reasonably performed with local lead. During cupellation, the Pb-Ag alloy was generally melted again at of 960–1000 °C in an oxidizing environment in order to produce lead monoxide (litharge), which was separated from metallic silver [42,43]. In such conditions, if a considerable amount of zinc was present in the alloy, it could burn (at or above its boiling point, around 900 °C) and form ZnO smoke. Exposure to this smoke for a prolonged period of time can cause fever, tremors, and other unpleasant symptoms (known as "zinc chills" or "metal-fume fever") [44]. Moreover, metallic Pb and Zn are practically immiscible liquids, whereas Ag and Zn are partially miscible, thus the zinc partitioned preferentially into metallic silver, rather than into lead. Zinc can be easily removed from a Zn-Ag solution if it is heated until the zinc vaporizes, leaving nearly pure silver, but this process (known as the Parkes process) was only patented in 1850 [45,46].

Summarizing the segregation of zinc in the slags far away from lead before the cupellation step should limit the unpleasant side effects related to ZnO fumes, and should reduce zinc impurities in the produced lead and silver, thereby improving the metal quality.

We still do not know the origin of the Al_2O_3 aggregates. The Al-rich minerals are uncommon in the Colline Metallifere territory [47], and the main natural α-Al_2O_3 phase (beryl) is a gemstone, which is unrealistic to employ in metallurgy. The only common

Al-rich minerals outcropping in southern Tuscany are the so called "alunite minerals" [48], which were known and exploited (in Frassine, Allumiere, and Monte Leo near Monterotondo Marittimo) in medieval times [47], mainly for the extraction of potash [10]. One uncommon connection between alunite minerals and metallurgical slags was found in the ancient book *De Re Metallica* (book VI) by Georgius Agricola [49], in which "burned alum" is mentioned among smelting "additamenta," probably analogous to the modern fluxes that, following the author, should include: reducing, oxidizing, sulfurizing, and collecting agents. In particular, there is a very complex recipe in which "alum reduced by fire to powder" is mentioned among many other ingredients in a fluxing mixture employed for lead separation ("But the most powerful flux is one which has two drachmae of sulphur and as much glass-galls, and half an uncia of each of the following, stibium, salt obtained from boiled urine, melted common salt, prepared saltpetre, litharge, vitriol, argol, salt obtained from ashes of musk ivy, dried lees of the aqua by which gold-workers separate gold from silver, alum reduced by fire to powder, and one uncia of camphor combined with sulphur and ground into powder. A half or whole portion of this mixture, as the necessity of the case requires, is mixed with one portion of the ore and two portions of lead, and put in a scorifier; it is sprinkled with powder of crushed Venetian glass, and when the mixture has been heated for an hour and a half or two hours, a button will settle in the bottom of the scorifier, and from it the lead is soon separated").

Following this suggestion, the observed α-Al_2O_3 phase found in slags could represent the product of thermal decomposition of alunite, which, during roasting above 750 °C, produces α-Al_2O_3, K_2SO_4, and SO_3 [50]. The observed α-Al_2O_3 aggregates could represent the waste remnants after alunite calcination and leaching for the recovery of potash [51], performed at some of the sites near Montieri, possibly Monteleo Allumiere [9,10], and re-employed as a fluxing agent in Zn-rich slags.

6. Conclusions

The considerable differences observed between the slags of the two studied sites are ascribable to the fact that different steps of the metallurgical process took place in the two sites, but also reflect the heterogeneity of the raw ores employed at the two sites.

Matte slags, which occurred in both the Cugnano and Montieri sites, represent the waste products of primary sulfide ore smelting aimed at obtaining a raw lead bullion. The distribution of these slags between a Ca-rich or Fe-rich dominant composition and the consequent mineralogy are tracers of the different ore-gangue association that occurred in the two areas.

The presence of silver was restricted to the small matte slags and ores enclosed within the mortar of the Montieri (Canonica) site. This suggest that wastes derived from the treatment of Ag-enriched mineral charges were finely crushed for the recovery of all Ag-rich matte/metals, and re-employed.

The other matte-poor slags are only associated with the Montieri territory, which suggests that a second step of smelting was performed only in this area due to the high zinc content of the ore charge. We suggest that raw lead matte/bullion obtained at Montieri was probably re-smelted, with fluxes, under more oxidizing conditions to reduce metal impurities. This second step was probably performed prior to Pb-Ag separation, or it was dedicated only to raw lead bullion from very impure ore.

The Al_2O_3-phases represent a sort of "fluxing agent" (possibly obtained from "burned alum") employed for Zn-rich lead ores. The segregation of zinc in the slags far away from lead, and before the cupellation step, should reduce zinc impurities and improve the metal quality.

Author Contributions: Conceptualization, L.C., M.B. and G.B.; methodology, L.C., L.D. and V.V.; field investigation, L.C., L.D. and V.V.; writing—original draft preparation, L.C.; writing—review and editing, L.C., V.V. and R.M.; project administration, G.B. and L.D.; funding acquisition, G.B. All authors have read and agreed to the published version of the manuscript.

Funding: This research was funded by nEU-Med (Origins of a new economic union (7th–12th centuries): resources, landscapes and political strategies in a Mediterranean region); and the European Research Council (ERC) under the European Union's Horizon 2020 research and innovation program (grant agreement n. 670792).

Institutional Review Board Statement: Not applicable.

Informed Consent Statement: Not applicable.

Data Availability Statement: Data is contained within the article.

Acknowledgments: We thank E.P., D.B., and T.C. for providing data and assisting us in our work. We are grateful to the entire nEU-Med research team for their kind assistance during the field work.

Conflicts of Interest: The authors declare no conflict of interest.

References

1. Francovich, R.; Parenti, R. *Rocca San Silvestro e Campiglia. Prime Indagini Archeologiche*; All'Insegna del Giglio: Florence, Italy, 1987; p. 208, ISBN 887-814-098-8.
2. Mascaro, I.; Benvenuti, M.; Tanelli, G. Mineralogy Applied to Archaeometallurgy: An Investigation of Medieval Slags from Rocca San Silvestro (Campiglia M.Ma, Tuscany). *Sci. Technol. Cult. Herit.* **1995**, *4*, 87–98.
3. Benvenuti, M.; Bianchi, G.; Bruttini, J.; Buonicontri, M.; Chiarantini, L.; Dallai, L.; Di Pasquale, G.; Donati, A.; Grassi, F.; Pescini, V. Studying the Colline Metallifere Mining Area in Tuscany: An Interdisciplinary Approach. In Proceedings of the Research and Preservation of Ancient Mining Areas, Yearbook of the Institute Europa Subterranea, 9th International Symposium on Archaeological Mining History, MuSe-Trento, Trento, Italy, 5–8 June 2014; pp. 5–8.
4. Bianchi, G. Dominare e gestire un territorio. Ascesa e sviluppo delle 'signorie forti' nella Maremma toscana del Centro Nord tra X e metà XII secolo. *Archeol. Mediev.* **2010**, *XXXVII*, 93–103.
5. Bianchi, G.; Bruttini, J.; Grassi, F. Lo scavo della Canonica di san Niccolò a Montieri (Gr). *Not. Soprintend. Beni Archeol. Toscana* **2012**, *8*, 564–567.
6. Bianchi, G.; Dallai, L.; Guideri, S. Indicatori di produzione per la ricostruzione dell'economia di un paesaggio minerario: Le Colline Metallifere nella Toscana Medievale. In Proceedings of the V Congresso nazionale di Archeologia Medievale, Foggia-Manfredonia, Italy, 30 September–3 October 2009; pp. 638–643.
7. Dallai, L.; Francovich, R. Archaeologia di miniera ed insediamenti minerari delle Colline Metallifere grossetane nel Medioevo. In *Il Calore Della Terra: Contributo Alla Storia Della Geotermia in Italia*; Cataldi, R., Ciardi, M., Eds.; ETS: Pisa, Italy, 2005; pp. 126–142, ISBN 978-884-671-407-7.
8. Bianchi, G.; Bruttini, J.; Dallai, L. Sfruttamento e ciclo produttivo dell'allume e dell'argento nel territorio delle Colline Metallifere grossetane. In *Risorse Naturali e Attività Produttive: Ferento a Confronto con Altre Realtà, Proceedings of the II Convegno di Studi in Memoria di Gabriella Maetzke, Viterbo, Italy, 27–28 April 2010*; De Minicis, E., Pavolini, C., Eds.; Tipografia Agnesotti: Viterbo, Italy, 2011; pp. 249–281.
9. Dallai, L. L'allumiera Di Monteleo Nel Territorio Di Monterotondo Marittimo. *Mélanges l'École Française Rome-Moyen Âge* **2014**, *126*, 245–258. [CrossRef]
10. Dallai, L. *Lo scavo dell'Allumiera di Monteleo. Nuovi dati per la produzione dell'allume alunitico nel tardo Medioevo, In I Paesaggi Dell'allume Archeologia Della Produzione Ed Economia Di Rete (Alum Landscapes Archaeology of Production and Network Economy)*; Dallai, L., Bianchi, G., Romana Stasolla, F., Eds.; All'Insegna del Giglio: Sesto Fiorentino, Italy, 2020; pp. 115–129, ISBN 978-88-7814-989-2.
11. Lattanzi, P.; Benvenuti, M.; Costagliola, P.; Tanelli, G. An overview on recent research on the metallogeny of Tuscany, with special reference to the Apuane Alps. *Mem. Soc. Geol. It.* **1994**, *48*, 613–625.
12. Pratellesi, G. Studio Giacimentologico Delle Mineralizzazioni Argentifere Della Zona di Massa Marittima—Montieri (Grosseto). Unpublished Thesis, University of Florence, Florence, Italy, 1984.
13. Benvenuti, M.; Chiarantini, L.; Cicali, C.; Villa, I.M.; Volpi, V. La produzione d'argento nel distretto minerario di Montieri-Massa Marittima (Colline Metallifere, Toscana meridionale) Alcune considerazioni su dati recenti. In *Les Métaux Précieux en Méditerranée Médiévale: Exploitations, Transformations, Circulations, Proceedings of the Colloque International d'Aix-en-Provence, France, 6–8 October 2016*; Minvielle Larousse, N., Bailly-Maître, M.C., Bianchi, C., Eds.; Presses Universitaires de Provence: Aix-Marseille, France, 2019; pp. 41–51.
14. Haupt, T. *Esperienze Dell'interno dei Monti e Della Industria Delle Miniere, Annali di Miniere, 1*; Le Monnier: Florence, Italy, 1851; pp. 1–35.
15. Lotti, B. Il Poggio di Montieri (provincia di Grosseto). *Boll. Regio Com. Geol.* **1976**, *7*, 111–122.
16. Lotti, B. *Descrizione Geologico-Mineraria dei Dintorni di Massa Marittima in Toscana, Memorie Descrittive Della Carta Geologica D'italia*; Tipografia Nazionale: Rome, Italy, 1983.

17. Bruttini, J.; Fichera, G.; Grassi, F. Un insediamento a vocazione mineraria nella Toscana medievale: Il caso di Cugnano nelle Colline Metallifere. In Proceedings of the V Congresso nazionale di Archeologia Medievale, Foggia-Manfredonia, Italy, 30 September–3 October 2009; pp. 306–312.
18. Bianchi, G.; Bruttini, J.; Quiros Castillo, J.A.; Ceres, F.; Lorenzini, S.M. La lavorazione del metallo monetabile nel castello di Cugnano (Monterotondo M.mo): Lo studio delle aree produttive dei secoli centrali (XI-XII secolo). In Proceedings of the VI Congresso Nazionale di Archaeologia Medievale, L'Aquila, Italy, 12–15 September 2012; pp. 644–649.
19. Lisini, A. Le monete e le zecche di Volterra, Montieri, Berignone a Casole. *Riv. Numis. Ital.* **1909**, *22*, 253–302.
20. Villoresi, R. Classificazione cronologica delle emissioni medievali dei vari tipo monetali della zecca di Volterra. *Rass. Volterrana* **1994**, *70*, 153–170.
21. Volpe, G. *Medio evo Italiano*; Sansoni: Florence, Italy, 1961.
22. Bruttini, J.; Grassi, F. Archeologia Urbana a Montieri: Lo Scavo Dell'edificio de "Le Fonderie" in via Delle Fonderie. *FOLD&R FastiOnLine Doc. Res.* **2010**, *199*, 1–25.
23. Donaldson, C.H. An experimental investigation of olivine morphology. *Contrib. Mineral. Petrol.* **1976**, *57*, 187–213. [CrossRef]
24. Ströbele, F.; Wenzel, T.; Kronz, A.; Hildebrandt, L.H.; Markl, G. Mineralogical and Geochemical Characterization of High-Medieval Lead–Silver Smelting Slags from Wiesloch near Heidelberg (Germany)—An Approach to Process Reconstruction. *Archaeol. Anthropol. Sci.* **2010**, *2*, 191–215. [CrossRef]
25. Manasse, A.; Mellini, M. Chemical and Textural Characterisation of Medieval Slags from the Massa Marittima Smelting Sites (Tuscany, Italy). *J. Cult. Herit.* **2002**, 187–198. [CrossRef]
26. Costagliola, P.; Benvenuti, M.; Chiarantini, L.; Bianchi, S.; Di Benedetto, F.; Paolieri, M.; Rossato, L. Impact of Ancient Metal Smelting on Arsenic Pollution in the Pecora River Valley, Southern Tuscany, Italy. *Appl. Geochem.* **2008**, *23*, 1241–1259. [CrossRef]
27. Santarelli, S. Archeometallurgia delle scorie: Il sito medievale di Rocchette Pannocchieschi nel Territorio di Massa Marittima. Unpublished Thesis, University of Siena, Siena, Italy, 2000.
28. Hauptmann, A.; Pernicka, E.; Wagner, G.A. Untersuchungen zur Prozesstechnik und zum Alter der frühen Blei-Silbergewinnung auf Thasos. *Der. Anschnitt.* **1988**, *6*, 88–112.
29. Kresten, P. Melting points and viscosities of ancient slags: A discussion. *Hist. Metall.* **1986**, *20*, 43–45.
30. Ettler, V.; Cervinka, R.; Johan, Z. Mineralogy of Medieval slags from lead and silver smelting (Bohutín, PrÍbram District, Czech Republic): Towards Estimation Of Historical Smelting Conditions. *Archaeometry* **2009**, *51*, 987–1007. [CrossRef]
31. Hauptmann, A. *The Archaeometallurgy of Copper*; Springer: Berlin/Heidelberg, Germany; New York, NY, USA, 2007; ISBN 978-3-540-72237-3.
32. Osborn, E.F.; Muan, A. *Phase Equilibrium Diagrams of Oxide Systems*; Ceramic Foundation: Columbus, GA, USA, 1960.
33. Bachmann, H.G. *The Identification of Slags from Archaeological Sites*; Routledge: London, UK, 1982; ISBN 978-090-585-310-9.
34. Bachmann, H.G.; Lutz, C.; Thiemann, U. Schlackenviskositäten. *Der. Anschnitt.* **1989**, *7*, 137–140.
35. Rehren, T.; Schneider, J.; Bartels, C. Medieval lead-silver smelting in the Siegerland, West Germany. *Hist. Metall.* **1999**, *33*, 73–84.
36. Flament, J. Les Métallurgies Associées de la fin du XIIIe Siècle au XVe Siècle L'argent, les Cuivres et le Plomb à Castel-Minier (Ariège, France). Ph.D. Thesis, University of Orleans, Orléans, France, 2017. Available online: https://tel.archives-ouvertes.fr/tel-01956682/document (accessed on 1 December 2020).
37. Ettler, V.; Johan, Z.; Zavřel, J.; Selmi Wallisová, M.; Mihaljevič, M.; Šebek, O. Slag Remains from the Na Slupi Site (Prague, Czech Republic): Evidence for Early Medieval Non-Ferrous Metal Smelting. *J. Archaeol. Sci.* **2015**, *53*, 72–83. [CrossRef]
38. Martinón-Torres, M.; Freestone, I.C.; Hunt, A.; Rehren, T. Mass-Produced Mullite Crucibles in Medieval Europe: Manufacture and material properties. *J. Am. Ceram. Soc.* **2008**, *91*, 2071–2074. [CrossRef]
39. Lee, W.E.; Zhang, S. Melt corrosion of oxide-carbon refractories. *Int. Mater. Rev.* **1999**, *44*, 77–104. [CrossRef]
40. Zhao, B.; Hayes, P.C.; Jak, E. Phase Equilibria Studies in the System ZnO-"FeO"-Al_2O_3-CaO-SiO_2 Relevant to Imperial Smelting Furnace Slags: Part I. *Metall. Mater. Trans. B* **2010**, *41*, 374–385. [CrossRef]
41. Zhao, B.; Hayes, P.C.; Jak, E. Phase Equilibria Studies in the System ZnO-"FeO"-Al_2O_3-CaO-SiO_2 Relevant to Imperial Smelting Furnace Slags: Part II. *Metall. Mater. Trans. B* **2010**, *41*, 386–395. [CrossRef]
42. Craddock, P.T. *Early Metal Mining and Production*; Edinburgh University: Edinburgh, UK, 1995; ISBN 074-860-498-7/978-074-860-498-2.
43. Bayley, J. Medieval precious metal refining: Archaeology and contemporary texts compared. In *Archaeology, History and Science: Integrating Approaches to Ancient Materials*; Martinón-Torres, M., Rehren, T., Eds.; Routledge: London, UK, 2008; pp. 131–150, ISBN 159-874-340-6/978-1598743401.
44. Fosmire, G.J. Zinc toxicity. *Am. J. Clin. Nutr.* **1990**, *51*, 225–227. [CrossRef]
45. Percy, J. *The Metallurgy of Lead: Including Desilverisartion and Cupellation*; Jhon Murray: London, UK, 1870.
46. Tylecote, R.F. *A History of Metallurgy*; CRC Press: Boca Raton, FL, USA, 1992; ISBN 978-0-901462-88-6.
47. Cuteri, F.; Mascaro, I. *Colline Metallifere, Inventario del Patrimonio Minerario e Mineralogico, Aspetti Naturalistici e Storico-Archeologici*; Edizioni Regione Toscana: Florence, Italy, 1995.
48. Dill, H.G. The geology of aluminium phosphates and sulphates of the alunite group minerals: A review. *Earth Sci. Rev.* **2001**, *53*, 35–93. [CrossRef]
49. Agricola, G. *De Re Metallica, Translated from the First Latin Edition of 1556 by Herbert Clark Hoover and Lou Henry Hoover*; Dover Publications Inc.: New York, NY, USA, 1950.

50. Özacar, M.; Ayhan Sengil, I. Adsorption of reactive dyes on calcined alunite from aqueous solutions. *J. Hazard. Mater.* **2003**, *98*, 211–224. [CrossRef]
51. Fink, W.L.; Van Horn, K.R.; Pazour, H.A. Thermal decomposition of Alunite. *Ind. Eng. Chem.* **1931**, *23*, 1248–1249. [CrossRef]